


A high-throughput single cell-based antibody discovery approach against the full-length SARS-CoV-2 spike protein suggests a lack of neutralizing antibodies targeting the highly conserved S2 domain

Mengya Chai , Yajuan Guo, Liu Yang, Jianhui Li, Shuo Liu, Lei Chen, Yuele Shen, Yi Yang, Youchun Wang, Lida Xu and Changyuan Yu

Corresponding authors: Yi Yang, Beijing Biocytogen Co., Ltd, Beijing 101111, China. E-mail: benny.yang@bbctg.com.cn; Youchun Wang, Division of HIV/AIDS and Sex-transmitted Virus Vaccines, Institute for Biological Product Control, National Institutes for Food and Drug Control (NIFDC) and WHO Collaborating Center for Standardization and Evaluation of Biologicals, Beijing 102629, China. E-mail: wangyc@nifdc.org.cn; Lida Xu, College of Life Science and Technology, Beijing University of Chemical Technology, Beijing 100029, China. E-mail: xuld@mail.buct.edu.cn; Changyuan Yu, College of Life Science and Technology, Beijing University of Chemical Technology, Beijing 100029, China. E-mail: yucy@mail.buct.edu.cn

Abstract

Coronavirus disease 2019 pandemic continues globally with a growing number of infections, but there are currently no effective antibody drugs against the virus. In addition, 90% amino acid sequence identity between the S2 subunit of severe acute respiratory syndrome coronavirus 2 (SARS-CoV-2) and SARS-CoV S proteins attracts us to examine S2-targeted cross-neutralizing antibodies that are not yet well defined. We therefore immunized RenMab mice with the full-length S protein and constructed a high-throughput antibody discovery method based on single-cell sequencing technology to isolate SARS-CoV-2 S-targeted neutralizing antibodies and cross-neutralizing antibodies against the S2 region of SARS-CoV-2/SARS-CoV S. Diversity of antibody sequences in RenMab mice and consistency in B-cell immune responses between RenMab mice and humans enabled screening of fully human virus-neutralizing antibodies. From all the frequency >1 paired clonotypes obtained from single-cell V(D)J sequencing, 215 antibodies with binding affinities were identified and primarily bound S2. However, only two receptor-binding domain-targeted clonotypes had neutralizing activity against SARS-CoV-2. Moreover, 5' single-cell RNA sequencing indicated that these sorted splenic B cells are mainly plasmablasts, germinal center (GC)-dependent memory B-cells and GC B-cells. Among them, plasmablasts and GC-dependent memory B-cells were considered the most significant possibility of producing virus-specific antibodies. Altogether, using a high-throughput single cell-based antibody discovery approach, our study highlighted the challenges of developing S2-binding neutralizing antibodies against SARS-CoV-2 and provided a novel direction for the enrichment of antigen-specific B-cells.

Keywords: SARS-CoV-2, SARS-CoV, neutralizing antibody, single-cell sequencing

INTRODUCTION

Coronavirus disease 2019 (COVID-19), caused by the severe acute respiratory syndrome coronavirus 2 (SARS-CoV-2), has been declared a global pandemic by the World Health Organization [1]. As of 22 June 2021, there have been more than 178 million confirmed cases with COVID-19 and 3.8 million deaths [2]. Now, these contagious viral mutants are continuing to spread repeatedly worldwide. SARS-CoV-2 is a single-stranded RNA virus and belongs to the lineage B of the genus

beta-coronavirus in the coronaviridae family together with SARS-CoV emerged in 2002, and both viruses share approximately 82% genomic similarity overall [3]. Numerous efforts have been made to characterize symptoms, immune cell profiling and treatment of COVID-19 [4–8]; however, just a handful of effective drugs for severe COVID-19 patients have emerged.

Neutralizing antibodies targeting the spike (S) glycoprotein are promising drug candidates for preventing or treating COVID-19. As a major component of the virus

Mengya Chai is a Ph.D. candidate in College of Life Science and Technology, Beijing University of Chemical Technology, Beijing 100029, China.

Yajuan Guo is a researcher in Institute for Antibody Therapeutic Innovation, Beijing Biocytogen Co., Ltd, Beijing 101111, China.

Liu Yang is a researcher in Institute for Antibody Therapeutic Innovation, Beijing Biocytogen Co., Ltd, Beijing 101111, China.

Jianhui Li is a researcher in Institute for Antibody Therapeutic Innovation, Beijing Biocytogen Co., Ltd, Beijing 101111, China.

Shuo Liu is a researcher in Division of HIV/AIDS and Sex-transmitted Virus Vaccines, Institute for Biological Product Control, National Institutes for Food and Drug Control (NIFDC) and WHO Collaborating Center for Standardization and Evaluation of Biologicals, Beijing 102629, China.

Lei Chen is a researcher in Institute for Antibody Therapeutic Innovation, Beijing Biocytogen Co., Ltd, Beijing 101111, China.

Yuele Shen is a researcher in Beijing Biocytogen Co., Ltd, Beijing 101111, China.

Yi Yang is a researcher in Institute for Antibody Therapeutic Innovation, Beijing Biocytogen Co., Ltd, Beijing 101111, China.

Youchun Wang is a professor in Division of HIV/AIDS and Sex-transmitted Virus Vaccines, Institute for Biological Product Control, National Institutes for Food and Drug Control (NIFDC) and WHO Collaborating Center for Standardization and Evaluation of Biologicals, Beijing 102629, China.

Lida Xu is an associate professor in College of Life Science and Technology, Beijing University of Chemical Technology, Beijing 100029, China.

Changyuan Yu is a professor in College of Life Science and Technology, Beijing University of Chemical Technology, Beijing 100029, China.

Received: November 27, 2021. Revised: January 25, 2022. Accepted: February 12, 2022

© The Author(s) 2022. Published by Oxford University Press. All rights reserved. For Permissions, please email: journals.permissions@oup.com

envelope, the coronavirus S glycoprotein is essential for receptor binding, fusion and virus entry and functions as a host immune defense target. The S protein comprises two functional subunits (S1 and S2): the S1 subunit at the N-terminal region facilitates viral attachment to the surface of target cells and contains the receptor-binding domain (RBD), and the S2 subunit is responsible for the fusion of the viral and host cell membranes. SARS-CoV-2 and SARS-CoV use the same angiotensin-converting enzyme 2 receptor bind with the RBD in the S1 subunit of S protein, and the S proteins of both viruses feature amino acid (AA) sequence identity around 76% and share a very similar structure [9, 10]. Therefore, most studies on screening neutralizing antibodies focused on the RBD [10–12]. The S2 domain of COVID-19 is not engaged in receptor binding; therefore, the neutralization potential of S2-specific antibodies is less appreciated in the field. Due to the fact that the S2 domain is a bit conserved among beta-coronaviruses, there is continued interest in the field to obtain broadly neutralizing antibodies against the relatively conserved S2 domain.

RenMab is a novel immunoglobulin (Ig) humanized mouse model developed on the C57BL/6 background (www.renmab.com). Heavy and kappa chain variable regions of the endogenous antibody gene loci were replaced *in situ* with human antibody genes while retaining the whole mouse constant (C) region. Recently, using RBD-immunized RenMab mice, Nie *et al.* have screened out potent neutralizing antibodies against SARS-CoV-2 and reported three epitope-distinct antibody cocktails that cooperatively eliminated the escape of virus mutants [13]. We hypothesized that similar methodologies immunizing RenMab mice with the full-length S protein could lead to antibodies that include targeting S2.

On the other hand, recently rapidly developed high-throughput single-cell sequencing technology is confirmed as a powerful tool for isolating human neutralizing antibodies [14]. Single-cell RNA sequencing (scRNA-seq) data describe the gene expression profile of individual B cells at single-cell resolution, which is necessary for cell identification; while single-cell V(D)J sequencing (scV(D)J-seq) of B cells enables us to obtain large-scale, natively paired antibody sequences, which provides the chance for rapid antibody discovery. Recently, an integrated technology platform has successfully accelerated antibody discovery by using single-cell sequencing as one of the technological improvements and all procedures within 78 days [15].

In this study, using the entire S protein as an immunogen, we developed a high-throughput protocol for rapid identification of fully human antibodies in RenMab mice based on 10X Genomics single-cell sequencing. First, we confirmed that B-cell immune responses in RenMab mice and humans were consistent and determined 309 clonotypes for binding affinity validation. Among 309 enriched clonotypes, 215 antibodies bound to the full-length S protein. Then, the high-resolution transcriptome

landscape revealed that sorted B cells contained five distinct clusters. Bioinformatics analysis of antibody sequences combined with identification of cell clusters corresponding to 215 positive antibodies indicated that plasmablasts and germinal center (GC)-dependent memory B-cells had higher probabilities of producing antigen-specific antibodies than GC B-cells. Next, we found that 215 full-length S protein-binding antibodies mainly targeted the S2 region using surface plasmon resonance (SPR) assays; however, none of the S2-targeting neutralizing antibodies were found. Overall, this study not only indicates S2-targeting neutralizing antibodies against SARS-CoV-2 are lacking but also can assist in enriching B cells that have more potential to produce specific antibodies by using marker genes of plasmablasts and GC-dependent memory B-cells.

MATERIALS AND METHODS

Immunization of RenMab mice

The tested RenMab mice, provided by Biocytogen (www.renmab.com), were housed in a pathogen-free environment from 6 to 8 weeks of age for immunization. All animal experiments were performed in strict accordance with the Guide for the Care and Use of Laboratory Animals of the People's Republic of China. In both projects, six male RenMab mice were first immunized three times with 60 μ g plasmid encoding the full-length SARS-CoV-2 protein at 3-week intervals. For the BBCTG3 project, the mice then underwent a boost immunization with SARS-CoV-2 S protein (R683A, R685A) (SPN-C52H4; ACROBiosystems) and CHO cells overexpressing SARS-CoV-2 S protein) on day 26 after the third immunization. For the BBCTG6 project, RenMab mice were then injected twice with His-tagged SARS-CoV S protein (SPN-S52H5; ACROBiosystems) and QuickAntibody-Mouse5W (KX0210041; KBQbio, China) on days 52 and 66 after the third immunization, respectively. Seven days after the penultimate immunization, serums were collected via the orbital veins to detect antibody titer in both projects.

Antigen-specific B-cell enrichment

The enrichment strategies consist of two major steps: microbead-based B-cell enrichment and flow cytometry-based antigen-specific B-cell sorting. In BBCTG3, B cells from immune splenocytes were enriched by negative selection of non-B cells (CD3 ϵ , CD4, CD8a, CD49b, Gr-1 and Ter119 positive) and IgM⁺ cells with Pan B cell isolation kit II (130-104-443; Miltenyi) and anti-mouse IgM microbeads (130-047-302, Miltenyi). In BBCTG6, splenic B cells were directly enriched by anti-mouse IgG1 and IgG2a + b microbeads (130-047-101; Miltenyi, 130-047-201; Miltenyi). Then, the cells were resuspended in fluorescence-activated cell sorting (FACS) staining buffer (phosphate buffered saline (PBS) supplemented with 2% FBS and 2 mM EDTA) and stained with a cocktail of antibodies at 4°C for 30 min. These antibodies contained anti-mouse CD8a APC-eFluor 780,

anti-mouse CD4 APC-eFluor 780, anti-mouse Ly-6G (Gr-1) APC-eFluor 780, anti-mouse F4/80 APC-eFluor 780, anti-human/mouse CD45R-PE-Cy7 and anti-mouse IgM PerCP-eFluor 710 (eBioscience), and IgG-APC (115-136-071; Jackson ImmunoResearch). In addition, cells were stained with SARS-CoV-2 S protein conjugated to phycoerythrin (PE) (ab102918, Abcam) and fluorescein isothiocyanate (ab102884; Abcam). Sorted antigen-specific B cells were rapidly processed for single-cell library constructions. For both samples, the cell viability exceeded 90%.

Library preparation and sequencing of scRNA-seq

The library for scRNA-seq was prepared using the 10X Chromium Next GEM Single Cell 5' Library & Gel Bead Kit according to the manufacturer's instruction (10X Genomics). In brief, the captured cells were lysed to release RNAs, which were barcoded by the reverse transcription process and further amplified to acquire sufficient 5' transcripts to construct cDNA libraries. Then, these libraries were sequenced on an Illumina Novaseq 6000 sequencer with PE150 technology.

ScRNA-seq data preprocessing

The raw sequencing files were preprocessed using the Cell Ranger software (v3.1.0) obtained from the 10X Genomics website (<https://support.10xgenomics.com/single-cell-gene-expression/software/downloads/latest>). There were three main steps in this analysis pipeline: sample demultiplexing, barcode counting and single-cell 5' unique molecular identifier counting. Through the cell ranger count options, reads were aligned to the mouse reference genome mm10-3.0.0 and converted to a feature-barcode matrix.

Unsupervised clustering analysis

The Seurat package (v3.2.0) was used for downstream data aggregation, quality control, dimensionality reduction and clustering analyses of the filtered gene-barcode matrix [16]. We pooled the data from two mouse models by the *merge* function. Cells with fewer than 150 detected genes or unusually high proportions of mitochondrial gene expression were removed. After normalizing the remaining cells, the top 2000 high variable genes were identified using the *FindVariableFeatures* function and used for principal component analysis. Then, we selected significant principal components (PCs) covering the highest variance based on elbow plot and calculated clusters using the *FindClusters* function with a resolution = 0.1. For visualization, we used Uniform Manifold Approximation and Projection (UMAP) with the *RunUMAP* function. The PCs used in this step were the same as those used for the previous clustering.

ScV(D)J-seq and analysis

Full-length B-cell receptor (BCR) V(D)J segments were enriched from amplified 5' cDNA libraries using the 10X

Chromium Single-Cell V(D)J Enrichment kit according to the User Guide (10X Genomics). BCR sequencing data were assembled using Cell Ranger toolkit (v3.1.0) with cell ranger vdj pipeline. Given the characteristics of RenMab mice, we pre-built a customized reference genome humanVDJandmouseVDJC-3.1.0 that ensured the V(D)J segments (lambda chain excluded) aligned the human reference sequences while the C region sequences aligned to the mouse. After this pipeline was completed, we obtained rearranged full-length BCR V(D)J segments, complementary-determining region 3 (CDR3) sequences and clonotype frequency.

According to Change-O toolkit [17], the heavy and light chains of assembled BCR sequences were assigned to human germline sequences downloaded from the international ImmunoGeneTics information system [18] by IgBlast-1.12.0 [19]. Non-productive BCR sequences were discarded in the subsequent analysis. Then, R (v4.0.2) package alakazam [20] was used to perform CDR3 AA length and V and J gene usage preference analysis.

Clonal abundance and diversity

Clonal abundance and diversity analysis were performed by uniform resampling of the input sequences with 200 bootstrap realizations to correct variations in sequencing depth [21, 22]. All analyses were performed using R (v4.0.2) package alakazam [20]. Clonal abundance was estimated by a novel statistical framework of the complete clones-rank abundance distribution (RAD). This estimator combined the adjusted RAD for the clones detected in different cell clusters and the estimated RAD for the undetected clones to obtain the complete RAD estimator.

Clonal diversity was calculated by plotting the general diversity index (qD) over a range of diversity orders (q) [23]. To generate a smooth curve, D was calculated for each value of q from the minimum value (0) to the maximum value (4) incremented by 0.1.

Mutation analysis

Mutations include replacement (R) and silent (S) mutations. We measured the R mutation frequency of BCR heavy chain by comparing the entire input sequence to the germline sequence using Change-O [17].

Antibody expression and binding assays

The production of selected B-cell clonotypes began with DNA synthesis and vector construction. DNA fragments encoding variable regions were codon-optimized for human cell expression and synthesized by Tsingke Biotechnology. Heavy and kappa chains were cloned into PEE12.4 and PEE6.4 vectors (Lonza Biologicals), respectively. Then, plasmids containing heavy and kappa chains were cotransfected in the transient expression system of ExpiCHO-S™ cells (A29127; Thermo Fisher)

grown to 6×10^6 cells/ml by using ExpiFectamine™ CHO kit (A29129; Thermo Fisher). The supernatant was harvested on day 7 after transfection, and the antibodies were purified by protein A affinity chromatography on AKTA Avant (GE healthcare). Purified antibodies were further tested for binding to SARS-CoV-2 in flow cytometry and surface plasmon resonance (SPR) assays.

In flow cytometry experiments, 2×10^5 CHO cells over-expressing SARS-CoV-2 S protein were first seeded in 96-well plates. Then added 0.5 μg antibody and incubated for 30 min at 4°C. A 50 μl of 500-fold diluted secondary antibody anti-hIgG-Fc-Alexa Fluor 647 (109-606-170, Jackson ImmunoResearch) was added and incubated for another 30 min under the same conditions.

The binding affinities of purified antibodies to S2, RBD and S1 non-RBD of SARS-CoV-2 S protein were determined using SPR technology. Briefly, the antibodies were captured onto the protein A chip sensor chip (GE healthcare), and then serial dilutions of SARS-CoV-2 S2 (40590-V08B; Sinobiological), SARS-CoV-2 S1 (S1N-C52H4; Acrobiosystem) and SARS-CoV-2 RBD (40592-V08B, Sinobiological) flowed through the sensorchip system. A suitable pH value of 7.4 was used in the running buffer. The flow rate was 30 $\mu\text{l}/\text{min}$ with the binding time (association) set to 180 s, and the dissociation time was 600 s. Subsequently, Biacore 8K evaluation software (GE Healthcare) was used to conduct affinity fitting analysis on the generated data according to the 'Kinetics Affinity' model.

Pseudovirus neutralization assay

The SARS-CoV-2 pseudovirus was constructed using a vesicular stomatitis virus (VSV) pseudovirus production system as described previously [24]. Briefly, 15 ml Huh-7 cells with a $5\text{--}7 \times 10^5$ cells/ml concentration were prepared in a T75 cell culture flask and incubated overnight at 37°C, 5% CO₂. When the cell confluence reached 70–90%, we discarded the medium. Then, the cells were transfected with 30 μg plasmid expressing SARS-CoV-2 S protein and cultured at 37°C, 5% CO₂. At the same time, the cells were infected with 15 ml G*ΔG-VSV (VSV G-pseudotyped virus, Kerafast) to produce virus particles without an envelope. After 6–8 h, the supernatant was discarded, and the remaining cells were gently washed twice with PBS + 1% FBS. Next, 15 ml of fresh complete DMEM were added, followed by incubation for another 24 h until the cell supernatant containing pseudovirus was harvested.

The neutralization test was performed by incubating 50 μl SARS-CoV-2 pseudovirus [with a concentration of 1200 median tissue culture infective dose per milliliter (TCID₅₀/ml)] with 100 ml serial dilutions of the test samples in 96-well plates. Then, 100 μl (contains $2\text{--}3 \times 10^4$ cells) Huh-7 cells were added to each well and incubated at 37°C and 5% CO₂. After 24 h of incubation, we detected

the luminescence signal on a luminometer (PerkinElmer, Ensign).

RESULTS

Study design

The continuing fast spread of COVID-19 urges the need to develop more effective therapeutic pipelines. Because the full-length spike (S) glycoprotein on the viral surface is the main antigen that stimulates the body's immune system to produce neutralizing antibodies, we chose the SARS-CoV-2 S protein as the critical target for antibody discovery. The full-length S proteins of SARS-CoV-2 (1273 residues; strain Wuhan-Hu-1; GenBank: QHD43416.1) and SARS-CoV (1255 residues; strain Urbani; GenBank: AAP13441.1) share the receptor usage and have similar three-dimensional structures [10, 25]. Especially, the homology of primary AA sequences between both S protein S2 subunits, which play critical roles in the membrane fusion process via the six-helical bundle formed by the two-heptad repeat domain, is up to 90% (Figure 1A). However, RBD has been the focus in most neutralizing antibody discovery studies [10–12], and the S2 region is hardly concerned. Here, we sought to use the immunogen of full-length S protein, which provides more opportunities to obtain antibodies against different epitopes, to study whether these two antigens (SARS-CoV-2 S protein and SARS-CoV S protein) can induce cross-protective antibody responses against the conserved S2 domain.

We constructed two independent experimental protocols, named BBCTG3 and BBCTG6, respectively. In BBCTG3, RenMab mice were immunized three times with the plasmid encoding SARS-CoV-2 S protein followed by boosting with SARS-CoV-2 S protein (R683A, R685A)-overexpressing CHO cells. In BBCTG6, RenMab mice were immunized with the same form as in BBCTG3 for the first three times and then injected twice with His-tagged SARS-CoV S protein emulsified in QuickAntibody-Mouse5W adjuvant (Supplementary Figure 1 available online at <http://bib.oxfordjournals.org/>). As expected, RenMab mice elicit robust anti-SARS-CoV-2 antibody titers post-immunization (Supplementary Figure 2 available online at <http://bib.oxfordjournals.org/>). Then, the splenic IgG⁺ B cells were enriched by depleting non-B cells and IgM⁺ cells in BBCTG3, and IgG1/2a/2b⁺ B cells were positively enriched from the spleen in BBCTG6 (Supplementary Figure 1 available online at <http://bib.oxfordjournals.org/>). These enriched cells in both projects were further sorted to high purity by flow cytometry (Supplementary Figure 3 available online at <http://bib.oxfordjournals.org/>). Given that the number of antigen-reactive B cells or plasmablasts in each mouse is often limited, we pooled the sorted splenic B cells from six RenMab mice in each project and performed scRNA-seq and scV(D)J-seq using 10X Genomics. Then, we performed series of binding affinity and pseudovirus

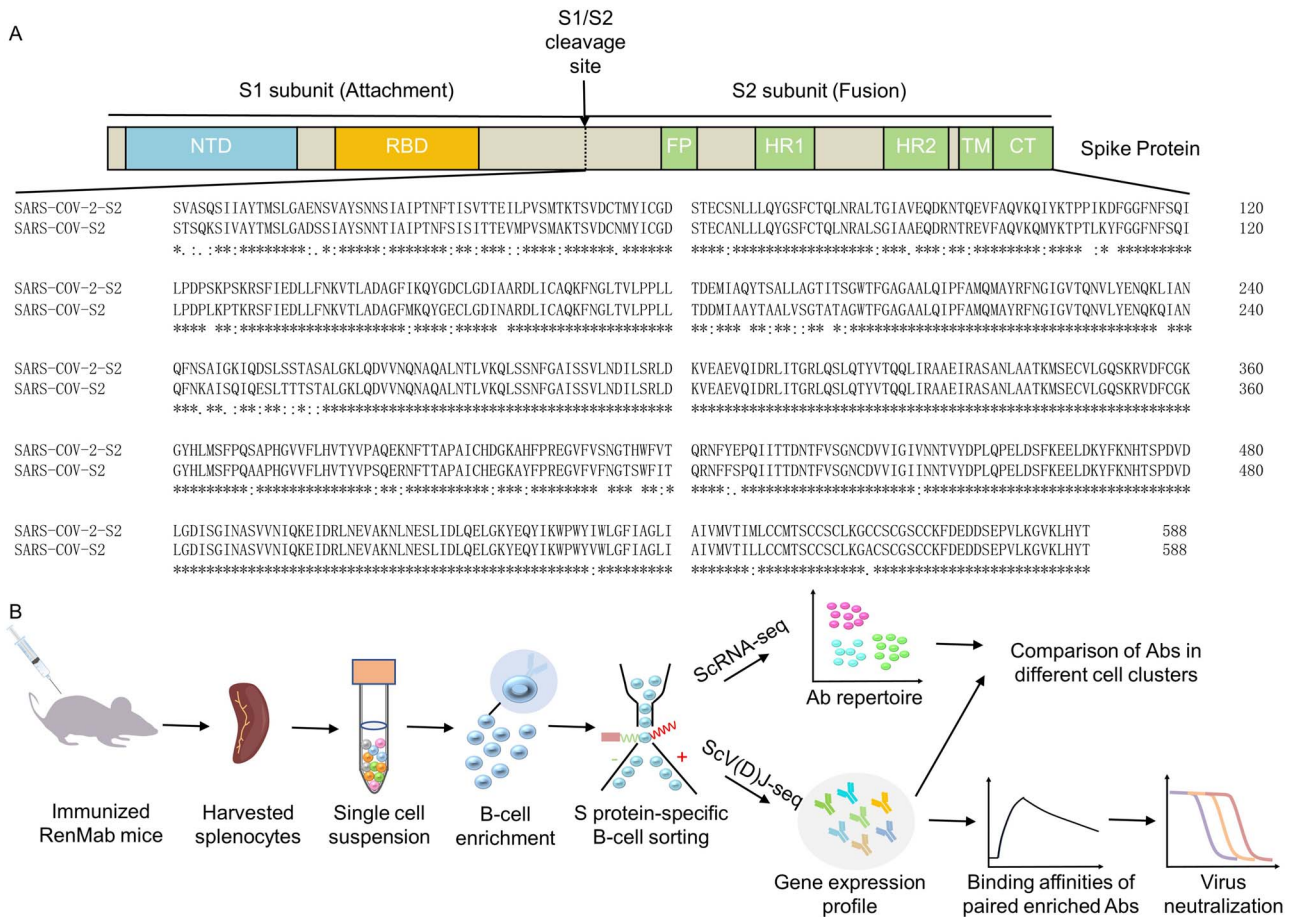


Figure 1. Study design for identifying the neutralizing antibodies against SARS-CoV-2 and its cross-neutralizing antibodies with SARS-CoV. **(A)** Sequence alignment of the S2 subunits of SARS-CoV-2 and SARS-CoV S proteins. **(B)** Schematic overview of each step in our study. We first isolated antigen-specific B cells from the spleen of immunized RenMab mice using magnetic beads and flow cytometry. Then, we used scV(D)J-seq and scRNA-seq to obtain natively paired heavy and light chain antibodies and cell types. Lastly, we performed a series of antibody binding and virus neutralization assays for enriched clonotypes to screen for neutralizing antibodies.

neutralization assays based on sequencing data. The general schematic design of this study is depicted in Figure 1B.

Rapid discovery of S protein-reactive antibodies by scV(D)J-seq

10X genomics-based high-throughput scV(D)J-seq enabled us to rapidly and accurately obtain full-length variable region sequences of naturally paired heavy and light chains for antibodies. So, we performed droplet-based scV(D)J-seq for sorted splenic B cells. Productive heavy and kappa chains obtained from BBCTG3 were 2451 and 3158 and from BBCTG6 were 2421 (productive heavy chain) and 3080 (productive kappa chain). We first analyzed CDR3 AA length, gene usage and V-J recombination preferences of these heavy and kappa chains to characterize the adaptive immune features of sorted B cells (Supplementary Figures 4 and 5 available online at <http://bib.oxfordjournals.org/>). As expected, we observed that CDR3 AA lengths of heavy chains were distributed more widely than that of the kappa chain (Supplementary Figures 4A and 5A), and V and J

genes involved various germline genes (Supplementary Figures 4B–D and 5B and C available online at <http://bib.oxfordjournals.org/>). Notably, there was a rather obvious preferential usage of the IGHV3 family, mostly rearranged with IGHJ4 or IGHJ6 (Supplementary Figure 4B and E available online at <http://bib.oxfordjournals.org/>). Interestingly, a similar B-cell immune response signature was observed in several studies on COVID-19 patients; especially, both RenMab mice and COVID-19 patients represented the repeated use of IGHV3-30 subfamily, while IGHV3-7 and IGHV3-23 that remarkably biased in COVID-19 patients were not significant in RenMab mice [26–28]. The preferred IGKVs in RenMab mice were IGKV1-5 and IGKV3-20 with the strongest recombination of IGKV3-20-IGKJ2, indicated specifically related to the SARS-CoV-2 and SARS-CoV (Supplementary Figure 5C and D available online at <http://bib.oxfordjournals.org/>). These data suggest that humanized RenMab mouse model is a valuable tool for drug discovery of human-related diseases.

Then, we performed a more detailed analysis of the retrieved antibody sequences (Table 1). In brief, we obtained 2044 and 2174 cells with productive V-J

Table 1. Summary of the 10X scVDJ-seq of sorted splenic B cells in immunized RenMab mice

Project	Immunization	Enrichment antigen	VJ paired cells	Clonotypes	IGH-IGK paired clonotypes	Frequency >1 paired clonotypes	antibodies tested	Positive antibodies
BBCTG3	SARS-CoV-2 S DNA	SARS-CoV-2 S protein	2044	1125	1090	153	153	106
BBCTG6	SARS-CoV-2 S DNA + SARS-CoV S protein	SARS-CoV-2 S protein	2174	907	848	156	156	109

spanning pairs in BBCTG3 and BBCTG6 after quality filtering. Correspondingly, the antibody sequences detected in both projects were grouped into 1125 and 907 clonotypes, respectively. Each clonotype shares an identical nucleotide sequence for CDR3 regions of both heavy and light chains. Since the goal was to screen for neutralizing antibodies, we filtered out the clonotypes containing (1) unpaired heavy or light chain; (2) two or more heavy and light chains simultaneously (the antibody cannot be accurately estimated as a certain type). After filtering, we obtained 1090 (BBCTG3) and 848 (BBCTG6) IG heavy and kappa chain (IGH-IGK) paired clonotypes. Among them, frequency >1 IGH-IGK paired clonotypes were 153 and 156 in both projects. Antigen-specific B cells would undergo BCR-mediated clonal expansion after repetitive antigenic stimulation, indicating that high-frequency clonotypes were more likely to produce high binding affinity and neutralizing antibodies against the antigen [29]. Thus, all the enriched 309 IGH-IGK paired clonotypes with frequencies greater than one were chosen as antigen-reactive antibody candidates for further characterization. We utilized FACS assays to check whether the tested antibodies could bind to SARS-CoV-2 full-length S protein, and 215 clonotypes were evaluated as positive. Of the 215 positive antibodies, the BBCTG3 project accounted for 106 and 109 for BBCTG6, yielding an overall positive rate of 70% for both projects.

Identification of sorted splenic B cells by scRNA-seq

To understand which cell subtypes are more likely to produce antigen-reactive antibodies, we determined the expression profile of sorted splenic B cells using scRNA-seq. Three thousand two hundred and sixty-seven cells from two projects were obtained after quality control described in 'Materials and Methods' section. These cells were classified into five clusters using the unsupervised clustering strategy (Figure 2A). The top seven marker genes of cell clusters were visualized as a bubble chart (Figure 2C). Combined with known B cell-related genes (Figure 2D and Supplementary Figure 6A available online at <http://bib.oxfordjournals.org/>), we identified GC B-cells, GC-dependent memory B-cells, plasmablasts and macrophage cells (Lyz2 and Fcgr1g). GC B-cells were proliferated and differentiated from activated B-cells, and landmark genes used to identify

the cluster include Aicda [which encode activation-induced cytidine deaminase that mediated class-switch recombination and somatic hypermutation (SHM)], Bach2, S1pr2 and Mki67 [30]. GC B-cells partially differentiated into memory B-cells during the immune response that highly expressed Ccr6, Cd38, Bcl2, Zeb2, Hhex, Gpr183 (for GC exit) and Ccr7 (for GC entry) [30, 31]. Since the existence of GC-independent memory B-cells that generated early in the immune response [32], the GC-derived memory B-cells in our study were defined as GC-dependent memory B-cells. Upon reimmunization, GC-dependent memory B-cells would be rapidly activated to produce plasmablasts or initiate secondary GC reactions [33]. Plasmablasts are short-lived antibody-secreting cells and annotated with Xbp1, Mzb1 and Jchain. In addition, we quantified the numbers of detected genes and transcripts of all cell types in RenMab mice (Supplementary Figure 6B and C available online at <http://bib.oxfordjournals.org/>), and cells with abnormally low genes and transcripts were defined as low-quality cells. Notably, cells from both projects exhibited similar global cell composition, although the absolute number of cells in each cell cluster of BBCTG3 was different from that in the BBCTG6 project (Figure 2B and Supplementary Figure 6D available online at <http://bib.oxfordjournals.org/>), indicating that activated B cells with specific immune responses to SARS-CoV-2 were consistent with those obtained from the mouse model that cross-immunized with SARS-CoV-2 and SARS-CoV.

Comparison of antibody sequences in different cell clusters

Based on the cell types mentioned above, we hypothesized that GC-dependent memory B-cells, GC B-cells and plasmablasts were the primary cell clusters to produce antibodies. Overall increased clonal abundance and reduced clonal diversity were observed in plasmablasts and GC-dependent memory B-cells compared to those in GC B-cells (Figure 3A and B), suggesting the former two cell populations exhibited more robust expansion than the latter. The positive selection of higher affinity B cells was generated through somatic hypermutation, and BCRs with increased mutations in CDRs corresponded to antigen-specific clones [34]. Indeed, higher replacement (R) mutation frequencies were presented in plasmablasts and GC-dependent memory B-cells (Figure 3C). Clonal

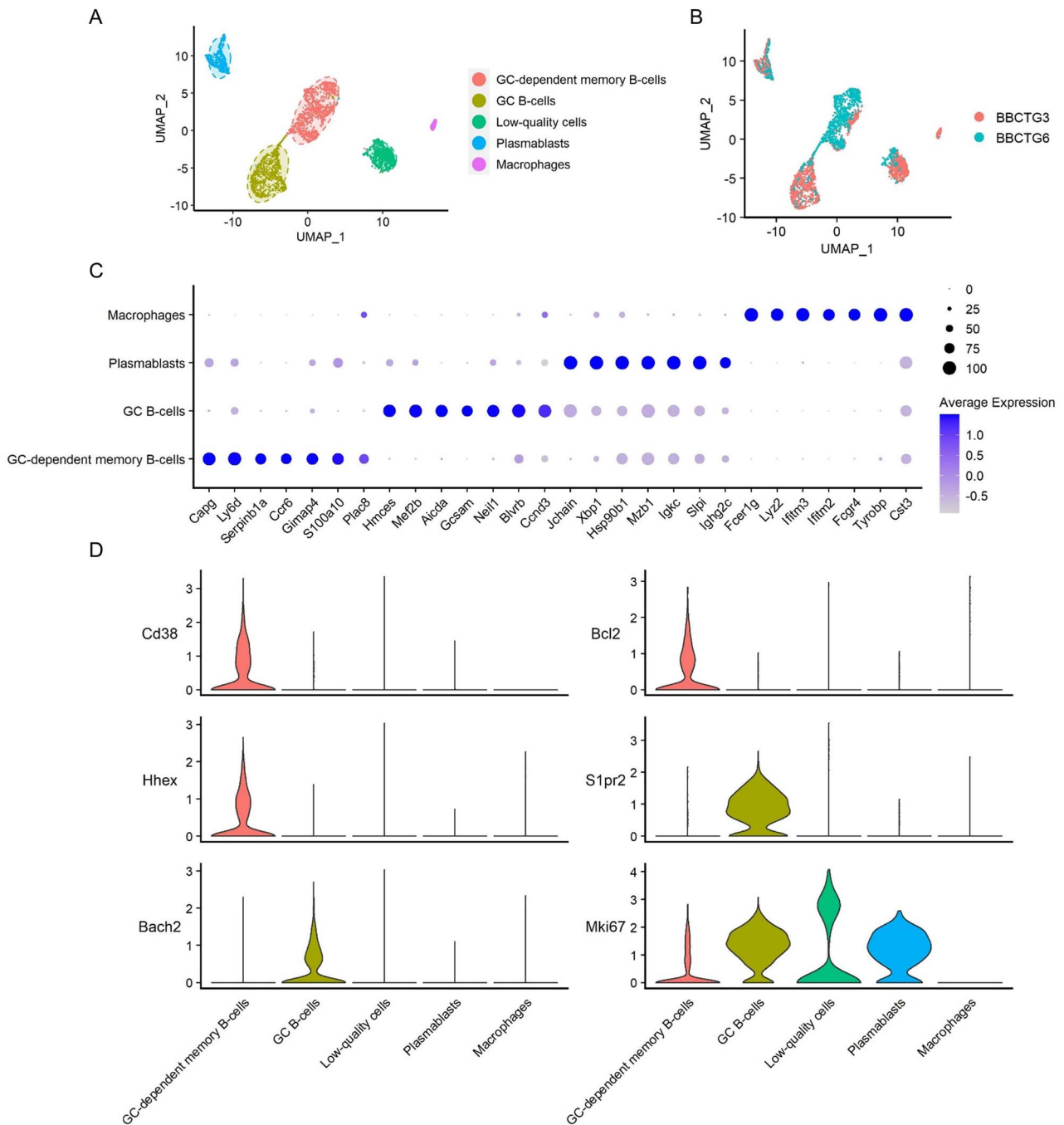


Figure 2. Analysis of single-cell transcriptome data in RenMab mice. (A, B) UMAP plots of $n = 3267$ splenic B cells are colored by cluster (A) and sample (B), respectively. (C) Expression of marker genes across identified cell clusters. (D) Violin plots show the expression levels of Cd38, Bcl2, Hhex, S1pr2, Bach2 and Mki67 used for cell typing.

frequency distributions revealed that the percents of BCRs with clonal frequencies greater than 1 were 63.5%, 47.2% and 38.5% in plasmablasts, GC-dependent memory B-cells and GC B-cells, respectively (Figure 3D). In addition, the experimental results further proved that the proportion of positive clones was decreased sequentially in plasmablasts, GC-dependent memory B-cells and GC B-cells (Figure 3E). Overall, we concluded that plasmablasts and GC-dependent memory B-cells have higher probabilities of producing antigen-specific antibodies than GC B-cells, and surface marker Sdc1

combined with Cd38 could be used for more effective antigen-specific B-cell enrichment.

Sequence analysis of full-length SARS-CoV-2 S positive antibodies

Based on understanding the cell types producing the positive clonotypes, we further characterized the sequences for 215 positive antibodies to assess the diversity of antigen-specific binding clonotypes discovered. The heavy chain V gene analysis of 215 positive antibodies revealed a significant IGHV3-30-3

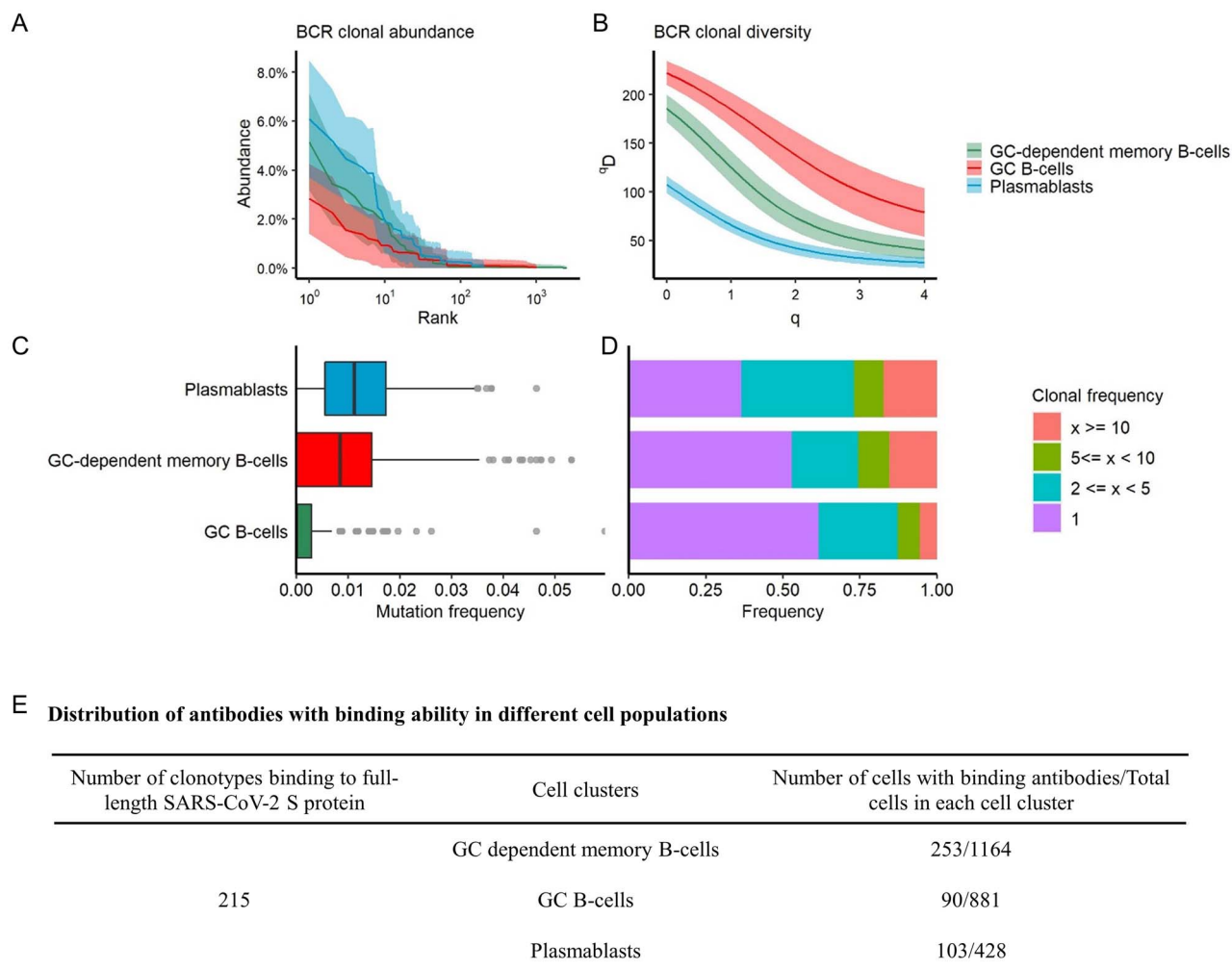


Figure 3. Comparison of plasmablasts, GC-dependent memory B-cells and GC B-cells at BCR level. **(A)** Clonal abundance. **(B)** Clonal diversity. **(C)** The replacement mutation frequency of heavy chain. **(D)** Clonal frequency distribution. **(E)** Distribution of the positive clones in different cell populations.

and IGHV3-30 preference (Figure 4A). Similarly, the antibodies isolated from convalescent COVID-19 patients showed strong enrichment in IGHV3-30-3 gene usage [35, 36]. And another research on COVID-19 patients revealed the overrepresentation of IGHV3-30 among the antibodies that bound the SARS-CoV-2 S trimer [37]. In addition, we found that IGKV1-5, IGKV3-20 and IGHJ6 were used repeatedly in immunized RenMab mice (Figure 4B and C). Among them, IGKV3-20 and IGHJ6 were significantly overexpressed in the antibodies isolated from COVID-19 patients [37]. Moreover, there was a diversity of CDR3 AA length (Figure 4D and E). Taken together, our results further indicated that antigen-reactive antibodies in RenMab mice are consistent with that in humans, and the repeated usage of IGHV3-30-3, IGHV3-30, IGKV3-20 and IGHJ6 provide the direction to discover potent neutralizing antibodies against SARS-CoV-2.

Epitope and antigen binding affinity among the positive antibodies

Next, the targeted epitopes of 215 positive antibodies were identified using SPR. 149 (68 + 81) of the positive

antibodies bound S2, 29 (26 + 3) bound RBD and 21 (11 + 10) bound S1 non-RBD. The remaining 16 antibody sequences, although identified as positive, showed no observable binding affinity to the above three domains. We calculated and displayed the association rate (on-rate, k_a) and dissociation rate (off-rate, k_d) of tested antibodies with SARS-CoV-2 S1/S2 in Figure 5A and B. Then, the equilibrium dissociation constant (K_D), which was determined as k_d/k_a , was used to analyze binding affinity. We observed that most positive sequences bound to SARS-CoV-2 S2 with K_D ranging from 2.45×10^{-9} M to 5.66×10^{-7} M, and S2-binding antibodies in BBCTG6 correspond to stronger affinity than those in BBCTG3 (Figure 5C). These results indicated that the antibody response was biased towards the S2 region when immunized with full-length S proteins.

Pseudovirus neutralization screening among the positive antibodies

Last, we examined the neutralization activity of 215 SARS-CoV-2 S-binding antibodies in a SARS-CoV-2 pseudovirus neutralization system. Among all the antibodies tested, two RBD-binding antibodies showed weak

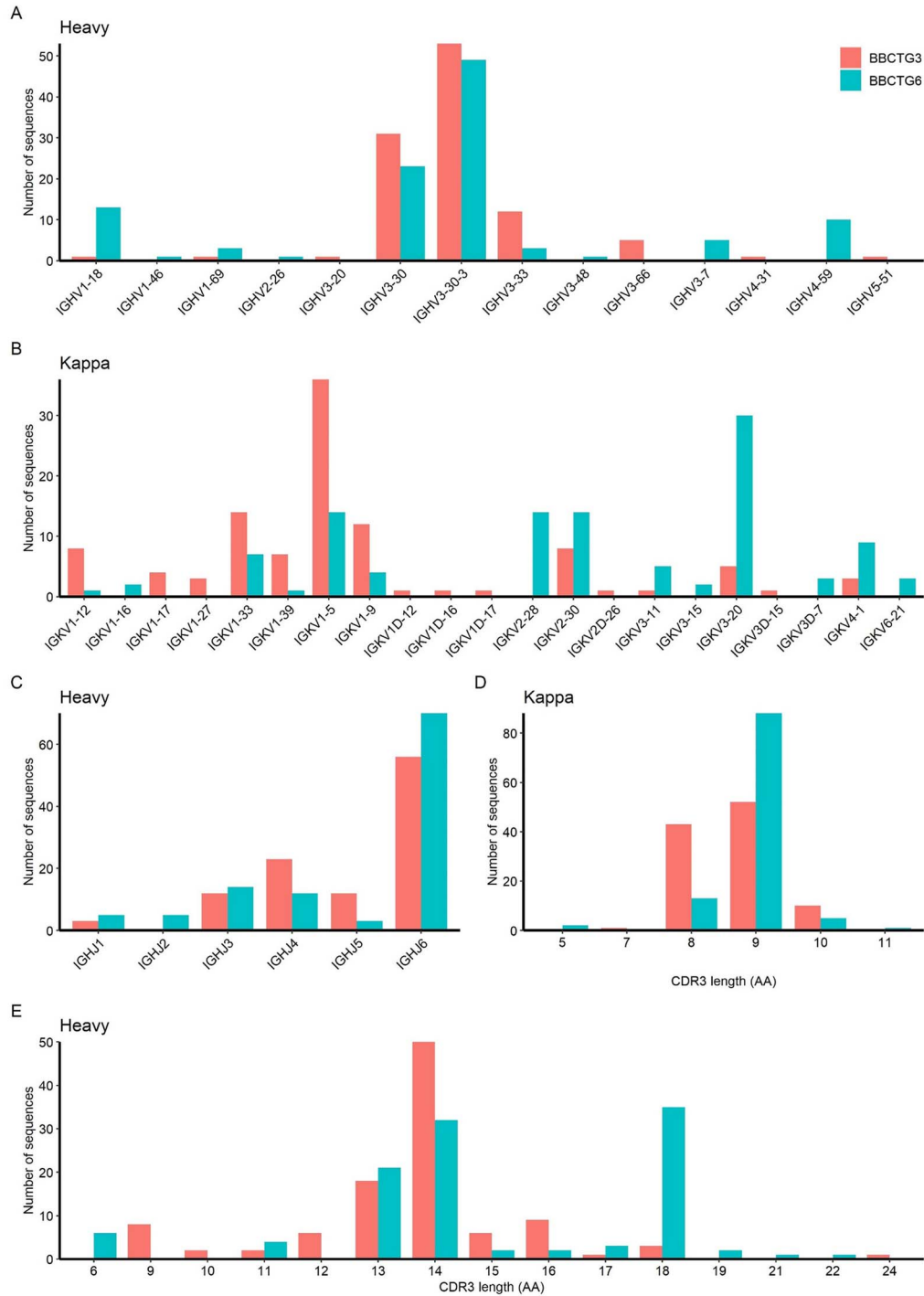


Figure 4. Sequence features of 215 positive antibodies binding to SARS-CoV-2 S protein. Germline gene distributions of IGHV (A), IGKV (B) and IGHJ (C). CDR3 AA lengths of kappa (D) and heavy chains (E). Red and blue represent BBCTG3 and BBCTG6, respectively.

neutralization ability with the half-maximal inhibitory concentrations (IC_{50}) values of 43.55 $\mu\text{g/ml}$ (BBCTG3) and 47.15 $\mu\text{g/ml}$ (BBCTG6), respectively (Figure 6). In addition, 16 positive but non-epitope-binding antibodies displayed no neutralization abilities (data not shown). Such phenomena were surprising because there were no S2-targeted neutralizing antibodies against SARS-CoV-2, although most antibodies isolated from the immunized

RenMab mice showed binding affinities for the S2 region.

DISCUSSION

Neutralizing antibodies are promising means to combat viral infection [38]. While traditional antibody-drug development methodologies is detrimental to cope with

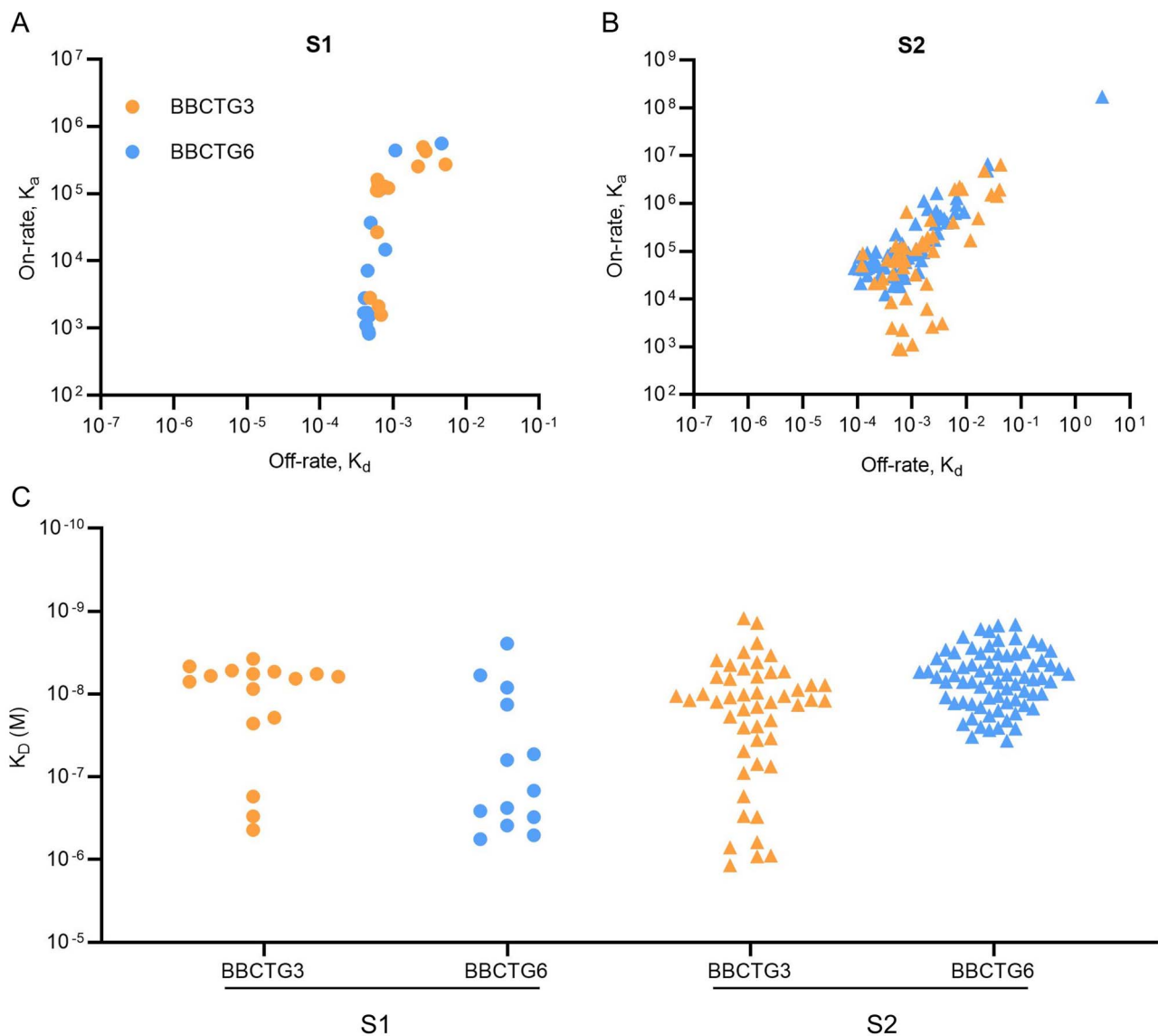


Figure 5. Binding affinities of antibodies to SARS-CoV-2 S1 or S2. (A, B) Association and dissociation constant of antibodies binding to S1 (A) or S2 (B). (C) Affinity equilibrium constant K_D of the tested antibodies.

SARS-CoV-2 because they usually take months or even years. To improve the efficiency of isolating neutralizing antibodies, we applied humanized mouse models and high-throughput single-cell sequencing technology in this study. Compared to human subjects, antibody repertoire-humanized mice could be immunized multiple times with the same or different viral immunogens in the presence of adjuvants, which eliminates the need for researchers to contact virus-infected individuals. These advantages enable us to isolate possible cross-neutralizing antibodies against several antigens through a mouse and explore future threats in advance. Moreover, mouse models are more readily available. Recently, a few studies have successfully obtained high-affinity antibodies by using humanized mouse models instead of peripheral blood mononuclear cells from the convalescent COVID-19 patients [13, 25, 39, 40]. RenMab model used in our study, to our knowledge, is the only genome

editing model carrying the entire human heavy and kappa chain variable regions. On the other hand, various methods currently exist for screening neutralizing antibodies from humans and mouse models. Hybridoma and in vitro display technology (such as phage and yeast display libraries) are the commonly used platforms. However, the efficiency of the former is low, and the latter tends to generate biased antibody repertoires and loses the native pairing information of heavy and light chains [41]. Optofluidics platform [such as Beacon (Berkley Light)] together with single-cell reverse transcription-polymerase chain reaction allows to obtain auto-paired antibody sequences in several days but with less B-cell screening throughput than single-cell sequencing [42, 43]. The microfluidic-based single-cell sequencing technology enables isolating naturally paired antibody sequences from up to 10000 B cells in one run, which any of the methods mentioned above cannot easily achieve.

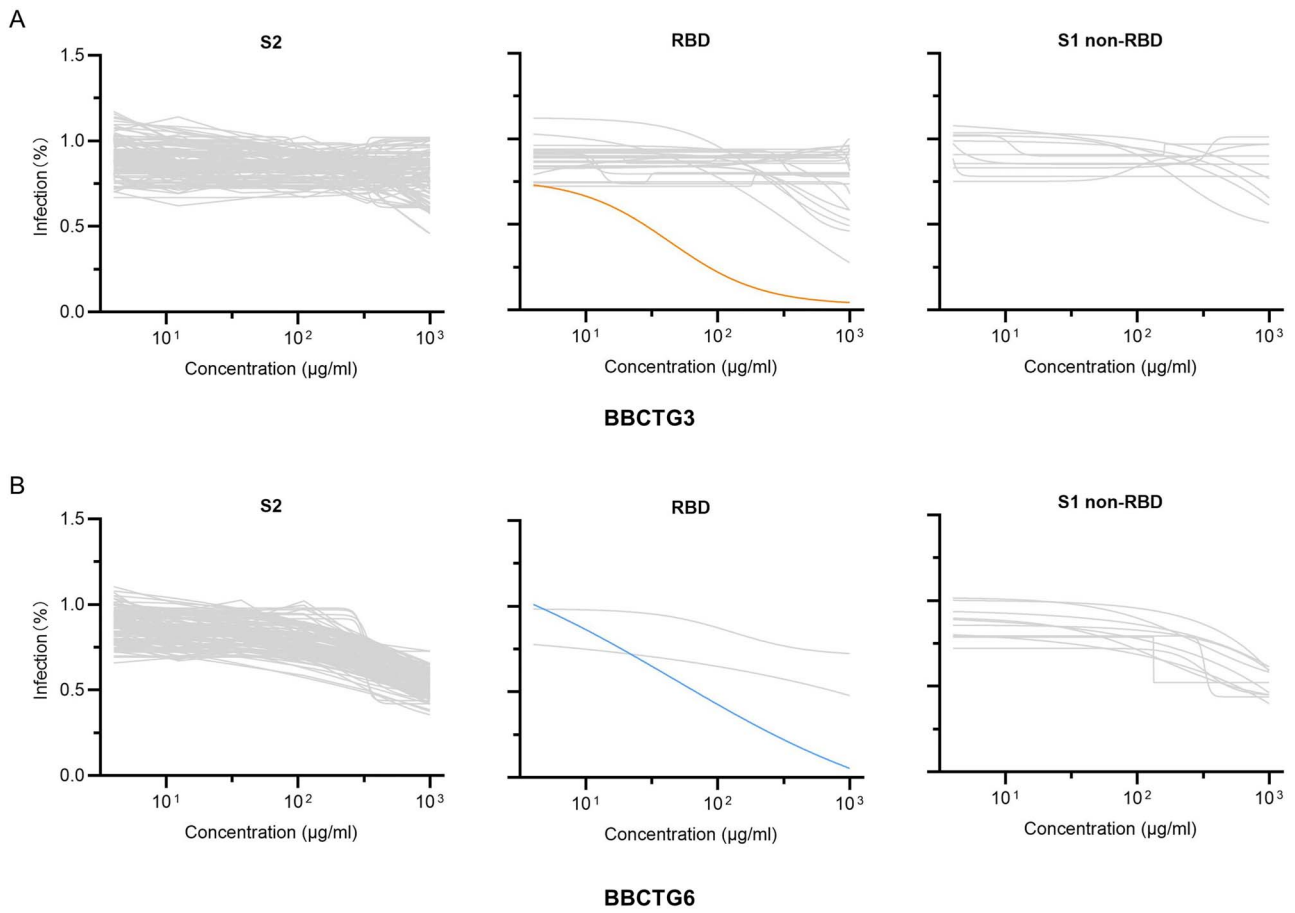


Figure 6. Neutralization potency of 199 purified antibodies on SARS-COV-2 pseudovirus. The best-fit pseudovirus on SARS-COV-2 pseudovirus neutralization curves are represented separately by binding domains in BBCTG3 (A) and BBCTG6 (B) projects.

In addition, the enrichment frequency of each clonotype can be identified, which is crucial for the priority selection of antigen-binding antibodies. Altogether, we established a systematic protocol for discovering neutralizing antibodies against SARS-CoV-2/SARS-CoV by immunizing RenMab mice with the full-length S protein, microbead-based enrichment and flow cytometry-based sorting of splenic B cells, single-cell sequencing, SPR and pseudovirus neutralization assays (Figure 1B). The complete procedure from collecting splenocytes from immunized RenMab mice to validate antibody sequences only took about a month. Additionally, the streamlined fully human antibody discovery strategy could greatly help intervene in other currently existing or emerging infectious viruses.

During cell sorting, only B cells bearing specific antigen-binding receptors on the cell surface were enriched. Indeed, the sorted cells mainly included GC-dependent memory B-cells, GC B-cells and plasmablasts representing different B-cell development states (Figure 2). Plasmablasts are rapidly produced by pathogen-specific memory B cells during the recall response [33] and their frequency increased in COVID-19 patients [44, 45]. GC-dependent memory B-cells correspond to classic long-lived memory B cells generated in the T cell-dependent GC reaction [46] and focus

on generating high-affinity somatic antibody mutants [47]. GC is an important site for clonal expansion, SHM and affinity selection of B cells, and GC B-cells can differentiate into memory cells or plasma cells [48]. By comparing clonal abundance, clonal diversity, mutation frequency, clonal frequency and antibody positive rate of these three cell populations, we found that plasmablasts and GC-dependent memory B-cells were preferred to produce S-specific antibodies in binding (Figure 3). Therefore, surface protein Sdc1 and Cd38 expressed in plasmablasts and GC-dependent memory B-cells can be used as markers to sort antigen-specific B cells; however, these results are limited to our study.

Since antigen-specific B cells are likely to undergo clonal expansion, we selected all the frequency >1 clonotypes obtained from scV(D)J-seq to perform FACS and SPR assays. We identified 215 clonotypes that bind to the SARS-CoV-2 full-length S trimer. Of these, 106 were isolated from BBCTG3, and 109 were from BBCTG6, yielding an overall positive rate of 70% for both projects (Table 1). This indicates that preferential selection of clonally enriched B-cell clonotypes is necessary to accelerate antibody discovery. The further analysis reported that most positive antibodies bound to S2 and some S2-binding antibodies with $nM K_D$ (Figure 5). We were excited

about such results because one of our goals was to screen for S2-targeted cross-neutralizing antibodies; however, we only found two RBD-binding neutralizing antibodies with weak activity ($IC_{50} > 10 \mu\text{g/ml}$) without S2-binding neutralizing antibodies (Figure 6). B cells enriched using S protein in convalescent COVID-19 patients revealed a consistent result; that is, although RBD-binding antibodies account for a low proportion of total ideal antibodies with 20%, only RBD-binding antibodies showed neutralizing ability [14]. These results are interesting, and more antibody structure analysis is needed to explore the results.

Although the discovery of cross-protective antibodies against coronavirus is not the most urgent at present, it is certainly meaningful for combating SARS-CoV-2 as well as its variants and other coronaviruses. The high level of sequence and structural homology between the S2 subunits of SARS-CoV-2 and SARS-CoV S proteins prompted us to test whether the immunized RenMab mice produce cross-neutralizing antibodies. Unexpectedly, no S2-targeted neutralizing antibodies were isolated from the expanded clonotypes. Because large-scale FACS, SPR and pseudovirus neutralization assays were performed for all the riched clonotypes obtained from high-throughput scV(D)J-seq, we reasonably concluded the lack of S2-targeted neutralizing antibodies against SARS-CoV-2. Similarly, several other studies showed that such efforts on obtaining broadly neutralizing antibodies against the relatively conserved S2 domain of beta-coronaviruses were fruitless [49, 50]. These data emphasize the difficulties and challenges of discovering S2-targeted cross-neutralizing antibodies against coronavirus even though the S2 AA sequence between SARS-CoV-2 and SARS-CoV is up to 90% identical. With regard to our efforts, glycosylation pattern of the soluble protein might not fully mimic that of viral S2 in natural infection that potentially impacted the mouse immune responses.

In conclusion, the technological advances of our workflow included immunization of fully human antibody RenMab mice and single-cell sequencing technology promise to the rapid identification of cells at the single B-cell level and high-throughput screening of antibodies. Among the five cell clusters of sorted splenic B cells, plasmablasts and GC-dependent memory B-cells induce a more robust immune response than GC B-cells. By using cell surface markers of plasmablasts (Sdc1) and GC-dependent memory B-cells (Cd38), it is expected to directly sort out antigen-specific B cells for antibody discovery and avoid complicated enrichment procedures in the future. On the other hand, we observed that no S2-binding antibody showed neutralizing activity against SARS-CoV-2 despite mouse immunization and cell enrichment using the full-length S protein ensured obtain antibodies with binding affinity to different epitopes. We believe that our findings, albeit limited at present, provide valuable information for developing effective antiviral drugs against SARS-CoV-2.

Key Points

- The B-cell immune responses in humanized RenMab mice immunized with full-length S proteins were characterized by single-cell sequencing data and compared with those in humans.
- A series of experimental data indicated a lack of neutralizing antibodies targeting the highly conserved S2 domain of SARS-CoV-2.
- The cell cluster having more potential to produce specific antibodies was pointed out.

Author contributions

L.X., C.Y., Y.W. and Y.Y. conceived, designed and supervised the experiments. M.C., Y.Y., L.X., Y.G., J.L., C.Y. and Y.S. wrote the manuscript. M.C., Y.G., L.Y., J.L., S.L. and L.C. performed the experiments. All of the authors have read and approved the final manuscript.

Data availability

Correspondence and request for materials should be addressed to C.Y. or L.X.

Supplementary data

Supplementary data are available online at <https://academic.oup.com/bib>.

Funding

State Key Laboratory of Pathogen and Biosecurity (Academy of Military Medical Science) (SKLPBS2138); National Natural Science Foundation of China (Grant No. 82174531); Shenzhen Science and Technology Project (JCYJ20180507183842516).

References

1. Phelan AL, Katz R, Gostin LO. The novel coronavirus originating in Wuhan, China: challenges for Global Health Governance. *JAMA* 2020;**323**(8):709–10.
2. WHO. Coronavirus Disease 2019 (COVID-19) Weekly Epidemiological Update and Weekly Operational Update. <https://www.who.int/emergencies/diseases/novel-coronavirus-2019> (23 June 2021, date last accessed).
3. Lv H, Wu NC, Tsang OT-Y, et al. Cross-reactive antibody response between SARS-CoV-2 and SARS-CoV infections. *Cell Rep* 2020;**31**(9):107725.
4. Pierce CA, Preston-Hurlburt P, Dai Y, et al. Immune responses to SARS-CoV-2 infection in hospitalized pediatric and adult patients. *Sci Transl Med* 2020;**12**(564):eabd5487.
5. Ni L, Ye F, Cheng ML, et al. Detection of SARS-CoV-2-specific humoral and cellular immunity in COVID-19 convalescent individuals. *Immunity* 2020;**52**(6):971–977.e3.
6. Long QA-O, Liu BZ, Deng HA-OX, et al. Antibody responses to SARS-CoV-2 in patients with COVID-19. *Nat Med* 2020;**26**(6):845–8.

7. Yu F, Du L, Ojcius DM, et al. Measures for diagnosing and treating infections by a novel coronavirus responsible for a pneumonia outbreak originating in Wuhan, China. *Microbes Infect* 2020;**22**(2): 74–9.
8. Hodgson SH, Mansatta K, Mallett G, et al. What defines an efficacious COVID-19 vaccine? A review of the challenges assessing the clinical efficacy of vaccines against SARS-CoV-2. *Lancet Infect Dis* 2021;**21**(2):e26–35.
9. Walls AC, Park YJ, Tortorici MA, et al. Structure, function, and antigenicity of the SARS-CoV-2 spike glycoprotein. *Cell* 2020;**181**(2):281–292.e6.
10. Wrapp D, Wang N, Corbett KS, et al. Cryo-EM structure of the 2019-nCoV spike in the prefusion conformation. *Science* 2020;**367**(6483):1260–3.
11. Yuan M, Wu NC, Zhu X, et al. A highly conserved cryptic epitope in the receptor binding domains of SARS-CoV-2 and SARS-CoV. *Science* 2020;**368**(6491):630–3.
12. Yang R, Lan J, Huang B, et al. Lack of antibody-mediated cross-protection between SARS-CoV-2 and SARS-CoV infections. *EBioMedicine* 2020;**58**:102890.
13. Nie JH, Xie JS, Liu S, et al. Three epitope-distinct human antibodies from RenMab mice neutralize SARS-CoV-2 and cooperatively minimize the escape of mutants. *Cell Discov* 2021;**7**(1):53.
14. Cao Y, Su B, Guo X, et al. Potent neutralizing antibodies against SARS-CoV-2 identified by high-throughput single-cell sequencing of convalescent patients' B cells. *Cell* 2020;**182**(1): 73–84.e16.
15. Gilchuk P, Bombardi RG, Erasmus JH, et al. Integrated pipeline for the accelerated discovery of antiviral antibody therapeutics. *Nat Biomed Eng* 2020;**4**(11):1030–43.
16. Butler A, Hoffman P, Smibert P, et al. Integrating single-cell transcriptomic data across different conditions, technologies, and species. *Nat Biotechnol* 2018;**36**(5):411–20.
17. Gupta NT, Vander Heiden JA, Uduman M, et al. Change-O: a toolkit for analyzing large-scale B cell immunoglobulin repertoire sequencing data. *Bioinformatics* 2015;**31**(20):3356–8.
18. Giudicelli V, Duroux P, Ginestoux C, et al. IMGT/LIGM-DB, the IMGT comprehensive database of immunoglobulin and T cell receptor nucleotide sequences. *Nucleic Acids Res* 2006;**34**(Database issue):D781–4.
19. Ye J, Ma N, Madden TL, et al. IgBLAST: an immunoglobulin variable domain sequence analysis tool. *Nucleic Acids Res* 2013;**41**(W1):W34–40.
20. Stern JN, Yaari G, Vander Heiden JA, et al. B cells populating the multiple sclerosis brain mature in the draining cervical lymph nodes. *Sci Transl Med* 2014;**6**(248):248ra107.
21. Chao A, Gotelli NJ, Hsieh TC, et al. Rarefaction and extrapolation with Hill numbers: a framework for sampling and estimation in species diversity studies. *Ecol Monogr* 2014;**84**(1):45–67.
22. Chao A, Hsieh TC, Chazdon RL, et al. Unveiling the species-rank abundance distribution by generalizing the Good-Turing sample coverage theory. *Ecology* 2015;**96**(5):1189–201.
23. Hill MO. Diversity and evenness: a unifying notation and its consequences. *Ecology* 1973;**54**(2):427–32.
24. Nie J, Li Q, Wu J, et al. Quantification of SARS-CoV-2 neutralizing antibody by a pseudotyped virus-based assay. *Nat Protoc* 2020;**15**(11):3699–715.
25. Wang C, Li WA-OX, Drabek DA-O, et al. A human monoclonal antibody blocking SARS-CoV-2 infection. *Nat Commun* 2020;**11**(1):2251.
26. Zhang F, Gan R, Zhen Z, et al. Adaptive immune responses to SARS-CoV-2 infection in severe versus mild individuals. *Signal Transduct Target Ther* 2020;**5**(1):156.
27. Wen W, Su W, Tang H, et al. Immune cell profiling of COVID-19 patients in the recovery stage by single-cell sequencing. *Cell Discov* 2020;**6**:31.
28. Schultheiss C, Paschold L, Simnica D, et al. Next-generation sequencing of T and B cell receptor repertoires from COVID-19 patients showed signatures associated with severity of disease. *Immunity* 2020;**53**(2):442–455.e4.
29. Murugan R, Buchauer L, Triller G, et al. Clonal selection drives protective memory B cell responses in controlled human malaria infection. *Sci Immunol* 2018;**3**(20):eaap8029.
30. Laidlaw BJ, Duan L, Xu Y, et al. The transcription factor Hhex cooperates with the corepressor Tle3 to promote memory B cell development. *Nat Immunol* 2020;**21**(9):1082–93.
31. Gatto D, Wood K, Brink R. EB12 operates independently of but in cooperation with CXCR5 and CCR7 to direct B cell migration and organization in follicles and the germinal center. *J Immunol* 2011;**187**(9):4621–8.
32. Cyster JG, Allen CDC. B cell responses: cell interaction dynamics and decisions. *Cell* 2019;**177**(3):524–40.
33. Quast I, Tarlinton D. B cell memory: understanding COVID-19. *Immunity* 2021;**54**(2):205–10.
34. Hershberg U, Uduman M, Shlomchik MJ, et al. Improved methods for detecting selection by mutation analysis of Ig V region sequences. *Int Immunol* 2008;**20**(5):683–94.
35. Robbiani DF, Gaebler C, Muecksch F, et al. Convergent antibody responses to SARS-CoV-2 in convalescent individuals. *Nature* 2020;**584**(7821):437–42.
36. Brouwer PJM, Caniels TG, van der Straten K, et al. Potent neutralizing antibodies from COVID-19 patients define multiple targets of vulnerability. *Science* 2020;**369**(6504):643–50.
37. Liu L, Wang P, Nair MA-O, et al. Potent neutralizing antibodies against multiple epitopes on SARS-CoV-2 spike. *Nature* 2020;**584**(7821):450–6.
38. Jiang S, Hillyer C, Du L. Neutralizing antibodies against SARS-CoV-2 and other human coronaviruses. *Trends Immunol* 2020;**41**(5):355–9.
39. Fu D, Zhang G, Wang Y, et al. Structural basis for SARS-CoV-2 neutralizing antibodies with novel binding epitopes. *PLoS Biol* 2021;**19**(5):e3001209.
40. Zhang C, Wang Y, Zhu Y, et al. Development and structural basis of a two-MAb cocktail for treating SARS-CoV-2 infections. *Nat Commun* 2021;**12**(1):264.
41. Saggy I, Wine Y, Shefet-Carasso L, et al. Antibody isolation from immunized animals: comparison of phage display and antibody discovery via V gene repertoire mining. *Protein Eng Des Sel* 2012;**25**(10):539–49.
42. Goldstein LD, Chen YJ, Wu J, et al. Massively parallel single-cell B-cell receptor sequencing enables rapid discovery of diverse antigen-reactive antibodies. *Commun Biol* 2019;**2**(1):304.
43. Horns F, Dekker CL, Quake SR. Memory B cell activation, broad anti-influenza antibodies, and bystander activation revealed by single-cell transcriptomics. *Cell Rep* 2020;**30**(3):905–913 e906.
44. Wildner NH, Ahmadi P, Schulte S, et al. B cell analysis in SARS-CoV-2 versus malaria: increased frequencies of plasmablasts and atypical memory B cells in COVID-19. *J Leukoc Biol* 2021;**109**(1):77–90.
45. De Biasi S, Lo Tartaro D, Meschiari M, et al. Expansion of plasmablasts and loss of memory B cells in peripheral blood from COVID-19 patients with pneumonia. *Eur J Immunol* 2020;**50**(9): 1283–94.
46. Takemori T, Kaji T, Takahashi Y, et al. Generation of memory B cells inside and outside germinal centers. *Eur J Immunol* 2014;**44**(5):1258–64.

47. Kaji T, Ishige A, Hikida M, et al. Distinct cellular pathways select germline-encoded and somatically mutated antibodies into immunological memory. *J Exp Med* 2012;**209**(11): 2079–97.
48. Zhang Y, Garcia-Ibanez L, Toellner KM. Regulation of germinal center B-cell differentiation. *Immunol Rev* 2016; **270**(1):8.
49. Zost SJ, Gilchuk P, Case JB, et al. Potently neutralizing and protective human antibodies against SARS-CoV-2. *Nature* 2020;**584**(7821):443–9.
50. Suryadevara N, Shrihari S, Gilchuk P, et al. Neutralizing and protective human monoclonal antibodies recognizing the N-terminal domain of the SARS-CoV-2 spike protein. *Cell* 2021;**184**(9):2316–2331.e15.